ARTICLE
PUBLISHED ONLINE: 28 OCTOBER 2012 | DOI: 10.1038/NCHEMBIO.1096
nature chemical biology

Redirecting cell-type specific cytokine responses with engineered interleukin-4 superkines

Ilkka S Junttila[1–3,11], Remi J Creusot[4,11], Ignacio Moraga[5–8,11], Darren L Bates[5–8,11], Michael T Wong[4], Michael N Alonso[9], Megan M Suhoski[9], Patrick Lupardus[5–8], Martin Meier-Schellersheim[10], Edgar G Engleman[9], Paul J Utz[4], C Garrison Fathman[4], William E Paul[1] & K Christopher Garcia[5–8]*

Cytokines dimerize their receptors, with the binding of the 'second chain' triggering signaling. In the interleukin (IL)-4 and IL-13 system, different cell types express varying numbers of alternative second receptor chains (γc or IL-13Rα1), forming functionally distinct type I or type II complexes. We manipulated the affinity and specificity of second chain recruitment by human IL-4. A type I receptor–selective IL-4 'superkine' with 3,700-fold higher affinity for γc was three- to ten-fold more potent than wild-type IL-4. Conversely, a variant with high affinity for IL-13Rα1 more potently activated cells expressing the type II receptor and induced differentiation of dendritic cells from monocytes, implicating the type II receptor in this process. Superkines showed signaling advantages on cells with lower second chain numbers. Comparative transcriptional analysis reveals that the superkines induce largely redundant gene expression profiles. Variable second chain numbers can be exploited to redirect cytokines toward distinct cell subsets and elicit new actions, potentially improving the selectivity of cytokine therapy.

Cytokines regulate key cellular functions including differentiation, proliferation, apoptosis and antiapoptosis[1], principally through dimerization of receptor subunits, which initiates intracellular JAK-STAT activation[2,3]. Most cytokines mediate stimulation by first interacting with a high-affinity cytokine-binding chain (usually designated 'α'), followed by low-affinity interaction with a receptor chain such as γc, gp130 or βc[4]. The ultimate potency of the cytokine at inducing signaling is determined by the efficiency, that is, the affinity, of recruitment of the second chain[5,6]. In many of these systems, different cell types express different amounts of the first and second chain[7]. Thus, manipulation of the binding parameters for second chain recruitment could potentially skew the activity of a cytokine toward certain cell types[8], potentially making these new engineered cytokines more specific and possibly less toxic and therefore therapeutically advantageous.

IL-4 is a classical four–α-helix–bundle cytokine whose primary binding chain is IL-4Rα[9,10]. The IL-4–IL-4Rα complex serves as a ligand for the second component of the IL-4 receptor, which for the type I receptor is γc and for the type II receptor is IL-13Rα1 (ref. 9). Formation of the IL-4–IL-4Rα–γc or IL-4–IL-4Rα–IL-13Rα1 complex on the cell surface activates intracellular signaling pathways, including the JAK-STAT and the PI3K-AKT pathways[9,11]. Recent resolution of the crystal structures of extracellular domains of the IL-4–bound type I and type II IL-4 receptors (**Fig. 1a**) showed that IL-4 sits between IL-4Rα and the second receptor chain and is in direct contact with the second receptor chain through binding surfaces on the D helix of the cytokine[6]. IL-4 binds IL-4Rα with very high affinity (K_D = ~10^{-10} M) through a highly charged interface[12], whereas the subsequent binding of the IL-4–IL-4Rα complex to either γc or IL-13Rα1 is of relatively low affinity[6,9,13,14]. The very high affinity of IL-4 for IL-4Rα means that in most instances the formation of the signaling complex is largely determined by the extent of expression of the second chain (or chains)[15]. The alternative second chains have different patterns of cellular expression, with γc being mainly expressed on hematopoietic cells and IL-13Rα1 mainly expressed on nonhematopoietic cells. Much of IL-4's regulatory activity is mediated by B cells and T cells that mainly express type I receptors, whereas its effector functions, in which it mimics IL-13, are largely mediated by cells that uniquely express the type II receptor and also respond to IL-13. Through its capacity to use both the type I and type II receptors, IL-4 is positioned to have a central role in regulatory functions (such as T_H2 differentiation, immunoglobulin class switching, dendritic cell maturation and macrophage activation) as well as effector functions (such as airway hypersensitivity and goblet cell metaplasia). However, these latter activities are physiologically induced mainly by IL-13, which is made in far larger amounts than IL-4. Further, as IL-13 cannot bind the type I receptor, which is dominantly expressed on hematopoietic cells, it has little or no 'regulatory' activity.

Pharmacologically, using IL-4 to regulate lymphocyte differentiation is complicated by its activity on nonhematopoietic cells through binding to the type II receptor and consequent effector function. There have been previous efforts to engineer IL-4 analogs[16], including the design of the antagonist Pitrakinra[17]. With the recent determination of the three-dimensional structures of the complete liganded type I and type II receptor ternary complexes (**Fig. 1a**), we sought to engineer agonist IL-4 variants that would have altered relative binding activities for the second chains of the type I and type II receptors. In principle, these superkines could have dose-dependent activities that allow optimal regulatory function while having reduced side effects.

Here we decouple the pleiotropy of IL-4 signaling through the engineering of type I and type II receptor–selective IL-4 superkines

[1]Laboratory of Immunology, National Institute of Allergy and Infectious Diseases, National Institutes of Health, Bethesda, Maryland, USA. [2]School of Medicine, University of Tampere, Tampere, Finland. [3]Fimlab Laboratories, Tampere, Finland. [4]Department of Medicine, Division of Immunology and Rheumatology, Stanford University School of Medicine, Stanford, California, USA. [5]Howard Hughes Medical Institute, Stanford University School of Medicine, Stanford, California, USA. [6]Department of Molecular and Cellular Physiology, Stanford University School of Medicine, Stanford, California, USA. [7]Department of Structural Biology, Stanford University School of Medicine, Stanford, California, USA. [8]Program in Immunology, Stanford University School of Medicine, Stanford, California, USA. [9]Department of Pathology, Stanford University School of Medicine, Stanford, California, USA. [10]Laboratory of Systems Biology, National Institute of Allergy and Infectious Diseases, National Institutes of Health, Bethesda, Maryland, USA. [11]These authors contributed equally to this work. *e-mail: kcgarcia@stanford.edu

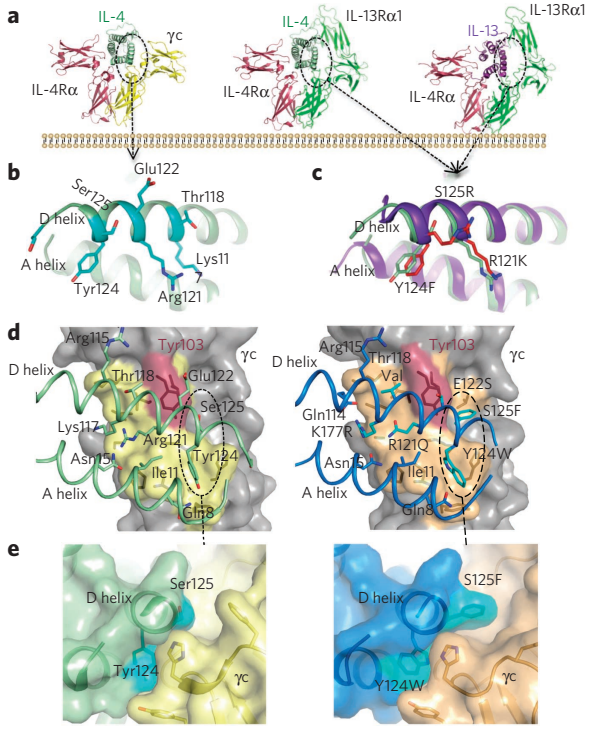

Figure 1 | Structure-based engineering of IL-4 superkines. (**a**) Crystal structures of the IL-4 and IL-13 type I and type II ternary ectodomain complexes[6]. (**b**,**c**) The principal γc and IL-13Rα1 binding sites on the D-helices of IL-4 and IL-13, respectively, as marked by dashed circles in **a**. The positions randomized in the IL-4 site 2 library are shown (**b**), and a structural superposition of IL-4 and IL-13 in the receptor complexes shows that positions 121, 124 and 125 of IL-4 superimpose closely on the analogous positions of IL-13 (**c**). In **c**, IL-13 is in purple, IL-4 is in light green and substituted residues are in red. (**d**) Isolated view of the site 2 interfaces in the wild-type IL-4 (left) and super-4 (right) complexes with γc. The view shown is the ribbon representation of the A and D helices of the cytokines, with γc-interacting side chains shown, projected onto the semitransparent molecular surface of γc. The interacting residues of γc underneath the surface are visible as dark outlines on the surface. The area contacted by the respective cytokines on γc is indicated in yellow on the surface, and the energetically critical Tyr103 of γc is colored red. (**e**) A dashed oval in **d** encircles a region of the interface shown from the side. In **e**, a close-up is shown of interface packing and shape complementarity in super-4 (right) versus IL-4 (left).

that show cell-type specificity and new activities, such as specific induction of dendritic cell maturation with a type II receptor-specific superkine. Remarkably, the structure-activity relationships of these superkines do not reveal a linear correlation between superkine potency and receptor affinity, and the highest-affinity superkines have a signaling advantage on cells with the lowest expression of second chain receptor chains. Thus, we demonstrate that cytokine affinity can be 'tuned' on the basis of second receptor chain expression to selectively target desired cell types and potentially improve the selectivity of cytokine therapy.

RESULTS

Development of high-affinity IL-4 variants

We used two different approaches to engineer IL-4 for higher-affinity binding to γc (**Fig. 1b**) or IL-13Rα1 (**Fig. 1c**): directed mutagenesis and *in vitro* evolution. To increase the affinity of IL-4 for γc, we took a combinatorial library approach and used yeast surface display[18] (**Supplementary Results**, **Supplementary Fig. 1a**). We produced C-terminally biotinylated ectodomains of IL-4Rα, γc and IL-13Rα1 for use as sorting reagents by coupling to streptavidin-phycoerythrin. We found that IL-4 displayed on yeast bound IL-4Rα with high affinity (**Supplementary Fig. 1a**) but did not bind γc in the absence of IL-4Rα (**Supplementary Fig. 1a**). In the presence of IL-4Rα, IL-4 on yeast binds the γc extracellular domain tetramer, indicating cooperative assembly of the heterodimeric receptor complex (**Supplementary Fig. 1a**). The use of high-avidity tetramers of γc was essential for the detection of the initial weak γc binding in the early rounds of library sorting. To create a library of D helix variants of IL-4, which is the principal γc-interacting helix of the cytokine (**Fig. 1b**), we inspected the IL-4–γc interface in the crystal structure of the type I receptor ternary complex. We created a focused library in which eight residues on the face of helix D were randomized (**Fig. 1b**), resulting in a yeast library with 2×10^8 variants. We carried out selections by decorating the yeast library with IL-4Rα to create the IL-4–IL-4Rα site 2 on the yeast and then sequentially enriched γc-binding yeast by decreasing the concentration of tetrameric, and finally monomeric, γc (**Supplementary Fig. 1b**). Sequencing the IL-4–selected variants revealed two unique sequences, the 'RQ' and 'RGA' variants, in which one, RGA, was highly enriched (**Supplementary Table 1**).

To increase the affinity of IL-4 for IL-13Rα1, we took a rational, structure-based approach rather than a combinatorial approach based on inspection of the site 2 interfaces formed by IL-4 and IL-13 with IL-13Rα1 (**Fig. 1c**). IL-13 binds with much higher affinity to IL-13Rα1 than IL-4 (K_D ~ 30 nM versus K_D > 1 μM)[6], so we aligned IL-4 with IL-13 from their structures in the two type II receptor ternary complexes (IL-4–IL-4Rα–IL-13Rα1 and IL-13–IL-4Rα–IL-13Rα1) to determine whether we could 'graft' important IL-13 receptor–interacting residues into the corresponding positions seen in IL-4 (**Fig. 1c**). We noted that three IL-4 D-helix residues, Arg121, Tyr124 and Ser125, which form important contacts with γc in the IL-4 type II receptor ternary complex, are substituted in IL-13 (ref. 6). We swapped these residues for their IL-13 positional equivalents (**Fig. 1c**) and made two IL-4 variants: a double mutant, R121K Y124F, referred to as KF, and a triple mutant, KFR, in which all three residues are swapped (R121K Y124F S125R).

Second receptor binding characteristics of the mutants

We expressed recombinant IL-4 and the variants KF, KFR, RQ and RGA using baculovirus and formed complexes with IL-4Rα to measure their binding affinities for IL-13Rα1 and γc by surface plasmon resonance (SPR; **Supplementary Table 1** and **Supplementary Fig. 2**). The K_D of wild-type IL-4–IL-4Rα for IL-13Rα1 and γc were 4,200 nM and 3,300 nM, respectively. KF–IL-4Rα had greater affinity for binding to both IL-13Rα1 (K_D = 250 nM) and γc (K_D = 330 nM). The addition of the S125R mutation in KFR resulted in a cytokine that had a 440-fold improvement over wild-type IL-4–IL-4Rα in affinity for IL-13Rα1 (K_D = 9.6 nM) but a decreased affinity for γc (K_D = 6,400 nM). In this respect, the grafting was highly successful and resulted in a three-log selectivity for IL-13Rα1 over γc.

The RQ and RGA variants complexed to IL-4Rα showed substantially higher affinity binding to γc (**Supplementary Table 1** and **Supplementary Fig. 2**). RQ–IL-4Rα showed a 36-fold higher affinity for γc (K_D = 91 nM), and RGA–IL-4Rα had a 3,700-fold higher affinity (K_D = 0.89 nM) than IL-4–IL-4Rα. Both RQ and RGA superkines showed substantially decreased binding to IL-13Rα1 (K_D = 29,000 nM and 21,000 nM, respectively) and would therefore be expected to have negligible type II receptor binding. The structure-based and *in vitro* evolution approaches have therefore yielded higher-affinity and receptor-selective IL-4 variants for functional testing. We refer to these cytokines as IL-4 superkines and specifically to the RGA variant as 'super-4'.

Structural basis of IL-4 affinity enhancement for γc

We sought to understand whether the super-4 docking mode with the second chain, γc, was perturbed relative to that of wild-type IL-4

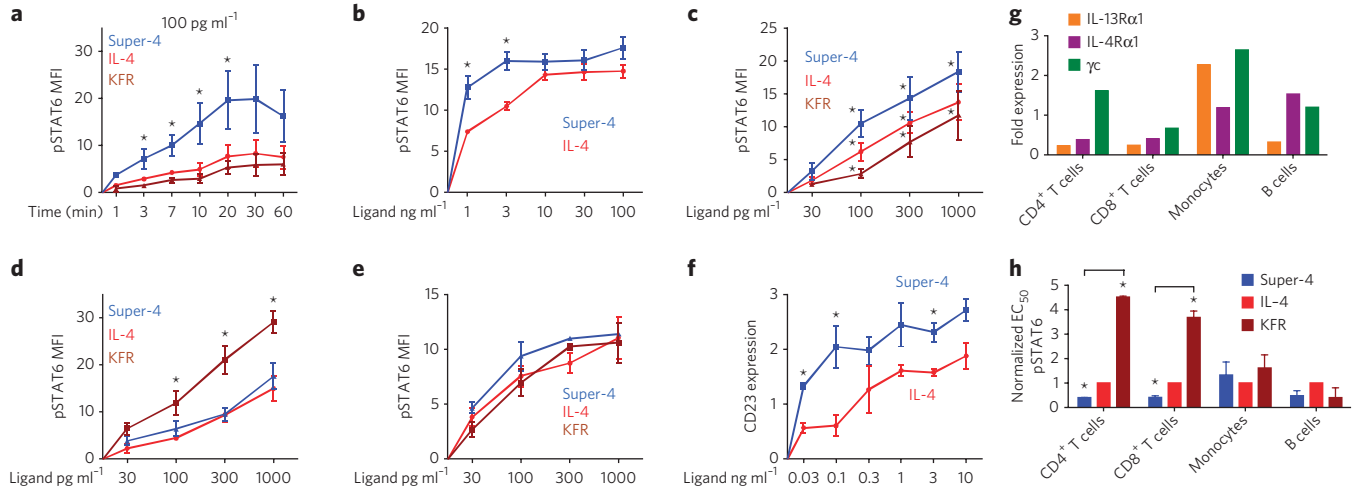

Figure 2 | Effect of IL-4 superkines on intracellular signaling. (**a**) Ramos cells starved overnight were unstimulated or stimulated for indicated times with 100 pg ml^{-1} of super-4, IL-4 or KFR. The cells were then fixed, permeabilized and stained with anti-pSTAT6. (**b**–**e**) Ramos cells (**b**), Ramos cell starved overnight (**c**), A549 cells (**d**) and U937 cells (**e**) were stimulated for 15 min with increasing amounts of IL-4, super-4 and KFR. The analysis was then performed as in **Figure 3a**. (**f**) Ramos cells were stimulated for 8 h either with IL-4 or super-4 as indicated, followed by surface staining of CD23. Mean ± s.e.m. from three independent experiments are shown for all experiments. (**g**) Expression of IL-4 type I and type II receptor chains on human PBLs from five donors. For the measurement of IL-4Rα, γc and IL-13Rα1 expression, B and T cells were gated by cell-surface markers (CD19, CD4 and CD8), whereas monocytes were identified as CD14$^+$ cells. Appropriate isotype controls served as a negative control. (**h**) Normalized pSTAT6 EC_{50} values obtained on the basis of sigmoidal dose-response curves of IL-4 and the superkines (**Supplementary Fig. 6**). pSTAT6 EC_{50} values from wild-type IL-4 were normalized to 1, and the EC_{50} values of the super-4 and KFR were calculated accordingly. Data are presented as mean ± s.d. Paired Student's *t*-test was used to determine significant changes. *$P < 0.05$ in all panels, obtained from the paired Student's *t*-test analysis.

because this issue is important in interpreting signaling activity differences. We were able to crystallize the binary super-4–γc complex in the absence of IL-4Rα and obtain a structure with a resolution of 3.25 Å (**Fig. 1d**,**e**, **Supplementary Table 2** and **Supplementary Fig. 3**). Superposition of the binary super-4–γc complex with the ternary type I signaling complex showed no major perturbations in cytokine-receptor orientation (**Supplementary Fig. 3a**,**b**). The position of γc bound to super-4 was essentially identical to the IL-4Rα–γc heterodimer geometry as observed in the complexes formed with wild-type IL-4. Therefore, any signaling changes we observe can most likely be attributed to increased affinity and not structural differences.

In the super-4–γc interface, side chain density was clear for super-4 D-helix residues 117–127 (**Supplementary Fig. 3c**); these engage the γc binding site in a topologically similar fashion to IL-4, with the γc hotspot residue Tyr124 occupying a central position (**Fig. 1d**). It seems clear that an important factor underlying super-4's enhanced affinity was the replacement of Ser125 with phenylalanine (**Fig. 1e**, left panel), which can insert into a large hydrophobic pocket of γc that was previously unoccupied, contributing an additional 52.5 Å^2 of buried surface area (**Fig. 1e**, right panel). The hydrophobic groove in γc occupied by IL-4 Tyr124 gained a hydrogen bond from the N7 of the tryptophan to a main chain carbonyl of γc. On the basis of the structure and SPR data, we propose that the major affinity gains in super-4 are derived from the R121Q, Y124W and S125F mutations. A detailed comparison of amino acid interactions of IL-4 and super-4 with γc is presented in **Supplementary Table 3** and **Supplementary Figure 3d**. We did not determine the structure of the KFR–IL-13Rα1 complex as the mechanism for affinity enhancement seems obvious from the structure analysis and engineering strategy. The three side chains substituted on the IL-4 D helix would endow IL-4 with 'IL-13–like' contacts.

Cell activation in response to IL-4 superkines

To study responses to IL-4 and its superkines, we used Ramos, HH, A549 and U937 cells. We first measured the relative expression of mRNA (**Supplementary Fig. 4a**) and protein (**Supplementary Fig. 4b**) of the type I and type II receptor chains on these cells. Ramos cells have large amounts of IL-4Rα, but their amounts of the type I receptor are limited by relatively low expression of γc. HH cells, although having less IL-4Rα than Ramos cells, have abundant γc. Both Ramos and HH cells have little or no IL-13Rα1. A549 cells have abundant type II receptor and little or no type I receptor. Finally, U937 cells have substantial amounts of both type I and type II receptor chains.

We initially tested the stimulatory activity of IL-4, super-4 and KFR. We used Ramos cells to study IL-4 responses dominated by the type I receptor complex (**Supplementary Fig. 4**). Stimulating Ramos cells with 100 pg ml^{-1} (~7 pM) of either IL-4, super-4 or KFR for various times, we found that the time course of stimulation of STAT6 phosphorylation by IL-4, super-4 and KFR is similar, but super-4 induces substantially more phosphorylation than does IL-4 or KFR at all of the time points measured (**Fig. 2a**); after 20 min of stimulation, the mean fluorescence intensity (MFI) of STAT6 phosphorylation induced by super-4, IL-4 and KFR is 19.6, 7.7 and 5.4, respectively. In addition, dose-response experiments performed in Ramos cells with the three cytokines showed that super-4 was ten-fold more potent than KFR, although the three cytokines reach the same 'plateau levels' of STAT6 phosphorylation (**Fig. 2b**,**c** and **Supplementary Fig. 5**). However, the relative advantage of super-4 over IL-4 was relatively modest in comparison with the ~3,700-fold difference in their solution equilibrium constants for γc when complexed to IL-4Rα (**Supplementary Table 1**).

A549 cells principally use IL-13Rα1 as their second chain (**Supplementary Fig. 4**). KFR was three- to ten-fold more stimulatory than IL-4; super-4 was indistinguishable from IL-4 (**Fig. 2d**). Again, there was a qualitative agreement that the highest-affinity superkine caused a better response, but the degree of signaling advantage by the variants did not mirror the absolute magnitudes of their difference in solution affinity. In U937 monocytes, which express both γc and IL-13Rα1, super-4 slightly outperformed IL-4, but the differences between the superkines and IL-4 were generally modest (**Fig. 2e**).

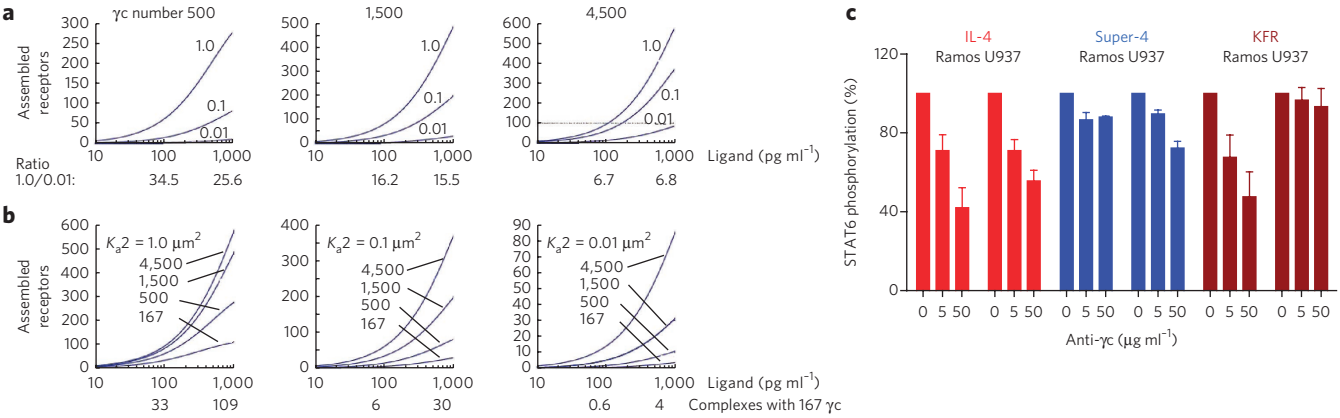

Figure 3 | Modeling of receptor assemblage in response to varying number of second chains. A Matlab algorithm was used to calculate assemblage of IL-4 receptors on cell surfaces expressing only the type I IL-4 receptor. (**a**) The IL-4Rα number was set to 1,500. The second chain number was raised from 500 to 4,500, and the K_a2 values of IL-4Rα complexes for the second chain ranged from 0.01 μm² to 1.0 μm² as indicated. The ratio of assembled chains of highest (1.0 μm²) versus lowest (0.01 μm²) second chain K_a2 values was calculated for 100 pg ml⁻¹ and 1,000 pg ml⁻¹ at 500, 1,500 and 4,500 γc molecules per cell. (**b**) The IL-4Rα number was set to 1,500. The K_a2 was varied from 1 μm² to 0.01 μm², and the second chain number was varied from 167 to 4,500 per cell. Complexes assembled with 167 γc chains per cell at 100 pg ml⁻¹ and 1,000 pg ml⁻¹ of IL-4 or superkines at K_a2 values of 1.0 μm², 0.1 μm² or 0.01 μm² are shown. (**c**) Phosphorylation of STAT6 in Ramos and U937 cells in response to IL-4, super-4 and KFR in the presence of anti-γc (0 μg ml⁻¹, 5 μg ml⁻¹ or 50 μg ml⁻¹). Response in the absence of anti-γc was normalized to 100%, and responses in the presence of anti-γc are expressed in relation to the normalized value. Data (mean ± s.e.m.) are from three independent experiments.

To investigate whether the superior STAT6 activation by super-4 results in the induction of STAT6-dependent gene products, we measured CD23 protein expression[19] in Ramos cells that had been stimulated for 8 h with either IL-4 or super-4. Super-4 was significantly ($P < 0.05$) more potent in inducing CD23 than IL-4 (**Fig. 2f**), but again, super-4 showed less of an advantage over IL-4 than might have been expected from its far greater capacity to bind γc when complexed to IL-4Rα.

Primary human cell responses to IL-4 and superkines

We next studied STAT6 phosphorylation responses of human peripheral blood leukocytes (PBLs) using Phospho-Flow cytometry coupled with fluorescent cell barcoding. We first measured IL-4Rα, γc and IL-13Rα1 expression in CD4 T cells, CD8 T cells, monocytes and B cells from five healthy donors by flow cytometry. IL-4Rα expression was highest on B cells, whereas monocytes had intermediate expression, and T cells had the least IL-4Rα (**Fig. 2g**). There was relatively little difference in γc expression between monocytes and CD4 T cells. B cells had slightly less γc, and CD8 T cells had the lowest amounts. As expected, IL-13Rα1 expression was highest on monocytes, whereas B and T cells had very low expression of this chain. PBLs were either unstimulated or stimulated with IL-4 or the various superkines for 15 min; STAT6 Tyr641 phosphorylation was measured by flow cytometry. Super-4 induced stronger phosphorylation of STAT6 than IL-4 and much stronger phosphorylation than KFR in CD4 and CD8 T cells (**Fig. 2h** and **Supplementary Fig. 6a–d**). Monocytes showed little difference in their responses to IL-4, super-4 and KFR, in keeping with their expression of both γc and IL-13Rα1.

Modeling of receptor assemblage

The notion that super-4 was only approximately three- to ten-fold more potent at activating STAT6 while its three-dimensional equilibrium constant for γc was ~3,700 times higher than that of IL-4 left us wondering how signal-inducing receptor formation is dictated by the expression of the second chain. To address this question, we used a Matlab script slightly modified from that used in our previous publication[7] (**Supplementary Methods**) to calculate the assemblage of receptor complexes as a function of ligand concentration upon varying second chain numbers and varying second chain equilibrium constants. This matrix takes into account three parameters: the surface expression of IL-4Rα and γc receptor chains, the alteration in two-dimensional binding affinities of ligand-bound IL-4Rα toward the γc chain and the ligand concentration. The calculation predicts the number of formed receptor complexes on the cell surface and does not directly describe signaling in particular as it assumes that the availability of intracellular signaling molecules (Jak1, Jak3, Tyk2 or STAT6) does not limit the complex formation. Further, the calculation assumes that the physical interaction between the cell membrane and all of the receptor chains involved is similar and limits the free movement of the receptor chain equally on the cell membrane.

As the number of IL-4Rα chains on Ramos cells has been reported to be ~1,500 (ref. 20), we determined the assemblage of receptors at this fixed IL-4Rα number. We used two equilibrium binding constants previously measured for the IFNα receptor as 'surrogate' values that would be expected to roughly correlate with type I and type II IL-4 receptors[21]. When the γc number was set to 4,500, there was a relatively modest effect of increasing the second chain two-dimensional equilibrium constant (K_a2) from 0.01 μm² to 1.0 μm². However, when the γc number was set to 500, the increase in the second chain K_a2 had a strong impact on the number of receptor chains assembled (**Fig. 3a**). Thus, with a cytokine concentration of 100 pg ml⁻¹, the ratio of assembled complexes for $K_a2 = 1$ μm² to $K_a2 = 0.01$ μm² was 6.7 when the number of second chains was 4,500, whereas that ratio was 34.5 when the γc number was set to 500. At 1,000 pg ml⁻¹, the $K_a2 = 1$ μm²/$K_a2 = 0.01$ μm² ratio for 4,500 γc molecules was 6.8, whereas it was 25.6 when the γc number was 500. Thus, increasing the second chain K_a2 becomes more useful when the second chain number is relatively low. This would effectively mean that a cell that expresses low numbers of γc or IL-13Rα1 would most strongly benefit from enhanced affinity in the second chain. Indeed, when we calculated the number of formed receptor complexes at 100 pg ml⁻¹ of ligand at only 167 γc receptor chains per cell, we found that the wild-type IL-4, with a two-dimensional K_a2 of 0.01 μm², assembled very few signaling complexes, as opposed to the 33 signaling complexes assembled by a superkine with a 100-fold higher two-dimensional K_a2 (**Fig. 3b**).

As IL-4 and super-4 stimulate STAT6 phosphorylation to reach similar plateau values (**Fig. 2b**), we reasoned that assembling more

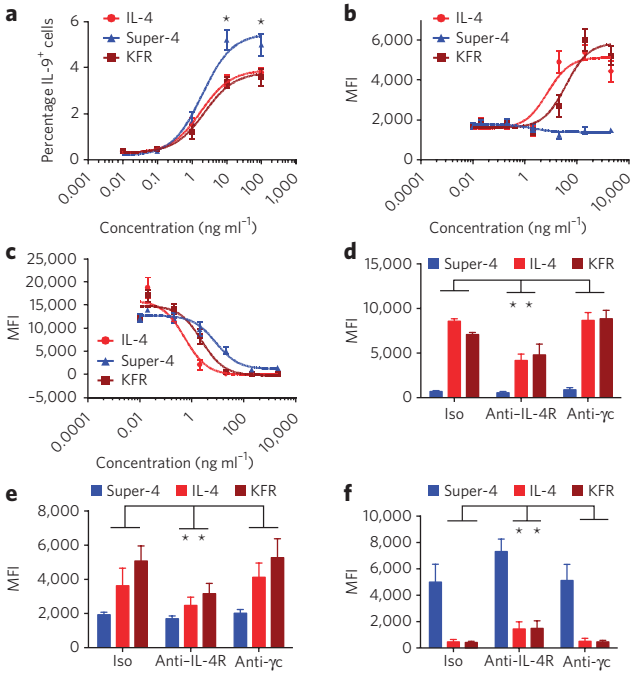

Figure 4 | Functional activities shown by IL-4 and superkines. (**a**) Human naïve $CD4^+CD45RA^+CD45RO^-CD25^-$ T cells were cultured with anti-CD3- and anti-CD28-coated beads in the presence of TGF-β and the indicated concentrations of IL-4, super-4 or KFR. Cells were subsequently analyzed for intracellular expression of IL-9. Data (mean ± s.e.m.) are from three independent experiments with more than four donors. (**b**,**c**) $CD14^+$ monocytes were isolated (>97% purity) from PBMCs obtained from healthy blood donors and cultured with 50 ng ml^{-1} GM-CSF alone or with the indicated concentrations of IL-4, super-4 or KFR. Cells were subsequently stained with DAPI, fluorescently labeled isotype control mAbs or mAbs against HLA-DR (**b**) and CD14 (**c**). Data (mean ± s.e.m.) are from three donors. (**d**–**f**) $CD14^+$ monocytes were isolated (>97% purity) and cultured with 50 ng ml^{-1} GM-CSF and 2 μg ml^{-1} of IL-4, KFR or super-4 in the presence of the indicated antibodies. Iso denotes the use of an isotype antibody as a negative control. Cells were processed and subsequently stained with DAPI, fluorescently labeled isotype control mAbs or mAbs against CD209 (**d**), CD86 (**e**) and CD14 (**f**). Data (mean ± s.e.m.) are from three donors. For all panels, $^*P < 0.05$; paired Student's *t*-test was used to determine significant changes.

signaling complexes than that induced by the lowest ligand concentration giving maximal stimulation would not result in any further signaling. As the plateau is achieved at 1,000 pg ml^{-1} of super-4 and 10,000 pg ml^{-1} of IL-4 in Ramos cells (**Fig. 2b**), we calculated the number of assembled complexes to be 65 for a ligand that had low affinity for the second chain (wild-type IL-4; 0.01 μm^2) using an intermediate number of γc chains (1,500) at 10,000 pg ml^{-1}.

Altering second receptor chain expression

Our modeling predicts that an increase in γc expression would be expected to decrease the advantage super-4 had over IL-4 and, conversely, that limiting availability of γc would lead to clearer differences between IL-4 and super-4. We studied the sensitivity to IL-4 and super-4 of the HH cell line, which had much higher expression of γc than Ramos cells (**Supplementary Fig. 4**). Super-4 was not superior to IL-4 or KFR in inducing phosphorylation of STAT6 in HH cells at concentrations ranging from 10 pg ml^{-1} to 10,000 pg ml^{-1} (**Supplementary Fig. 6e**).

An alternative test would be to diminish the accessibility of γc. For this purpose, we stimulated Ramos cells with 100 pg ml^{-1} of IL-4 or the super-4 and KFR superkines in the presence or absence of γc-specific antibody (anti-γc), measured the phosphorylation of STAT6 by flow cytometry and calculated the percentage decrease in STAT6 phosphorylation caused by anti-γc. STAT6 phosphorylation induced by IL-4 was decreased 58% by 50 μg ml^{-1} of anti-γc, whereas for that induced by super-4, the decrease was only 12% (**Fig. 3c**). For KFR, the inhibition was similar to that induced by IL-4. These results are consistent with the qualitative order of solution K_D values of IL-4 and the superkines for binding to γc (super-4 > IL-4 = KFR; **Supplementary Table 1**) and support the concept that increased affinity for the second chain results in greater stimulatory discrimination when the second chain expression is low.

In U937 cells, blocking γc would be predicted to diminish IL-4 responses, whereas there should be little impact on the activity of the KFR superkine because it principally uses the type II receptor. Indeed, blocking γc in U937 cells resulted in 44% reduction in STAT6 phosphorylation in response to IL-4 but only a 7% reduction in response to KFR (**Fig. 3c**).

Immunomodulatory activities of IL-4 superkines

To study the functional specificity and immunomodulatory abilities of IL-4 and the superkines, we performed a series of experiments involving CD4 T cells and monocytes (**Fig. 4**). The combination of TGF-β and IL-4 promotes the differentiation of naive human CD4 T cells into T_H9 cells[22]. To test whether super-4 more potently induces T_H9 differentiation than wild-type IL-4, naive $CD4^+CD45RA^+CD45RO^-CD25^-$ T cells were isolated from human PBL and cultured with beads coated with CD3- and CD28-specific antibody (anti-CD3 and anti-CD28) in the presence of TGF-β and varying concentrations of IL-4, super-4 or KFR for 4 d. Priming with 10 μg ml^{-1} or 100 μg ml^{-1} of super-4 resulted in a significantly ($P < 0.05$) higher percentage of cells that produced IL-9 upon subsequent stimulation with PMA and ionomycin than priming with the same concentrations of IL-4 or KFR (**Fig. 4a**).

IL-4, in combination with granulocyte macrophage colony-stimulating factor (GM-CSF), induces the *in vitro* differentiation of dendritic cells from human monocytes[23]. Highly purified monocytes were cultured with GM-CSF alone or with varying concentrations of IL-4, super-4 or KFR. After 6 d, cells were analyzed for cell-surface expression of the dendritic cell–associated molecules DC-SIGN (CD209), CD86 and HLA-DR. Notably, whereas IL-4 and KFR elicited monocyte differentiation into dendritic cells that expressed CD209, CD86 and HLA-DR (**Fig. 4b** and **Supplementary Fig. 7**), super-4 failed to do so, suggesting that such differentiation is mainly driven by signaling through the type II IL-4 receptor complex, which is poorly engaged by super-4. Furthermore, super-4 was somewhat less effective than KFR or IL-4 in downregulating CD14, a process also associated with the differentiation of monocytes into dendritic cells (**Fig. 4c**). Additionally, analysis of further markers used to distinguish different dendritic cell subsets show that cells induced by GM-CSF with or without super-4 are phenotypically identical (**Supplementary Fig. 8**), implying that super-4–induced cells were incompletely differentiated rather than differentiated into a distinct dendritic cell subset.

To confirm the relative roles of type I and type II IL-4 receptor complexes in dendritic cell differentiation, we showed that IL-4Rα-specific antibody (anti–IL-4Rα), which blocks both the type I and type II receptors, diminished the expression of CD86 and CD209 in response to IL-4 and KFR, whereas anti-γc, which only blocks the type I receptor, failed to do so (**Fig. 4d**–**f**). Super-4 caused very modest induction of these markers. Super-4–induced CD14 downregulation was partially inhibited by anti–IL-4Rα but not anti-γc. Thus, when γc was blocked, IL-4 and KFR still induced the same degree of dendritic cell maturation as in the control condition (**Fig. 4d**–**f**), confirming that the type II IL-4 receptor complex has an important role in GM-CSF– and IL-4–mediated dendritic cell differentiation.

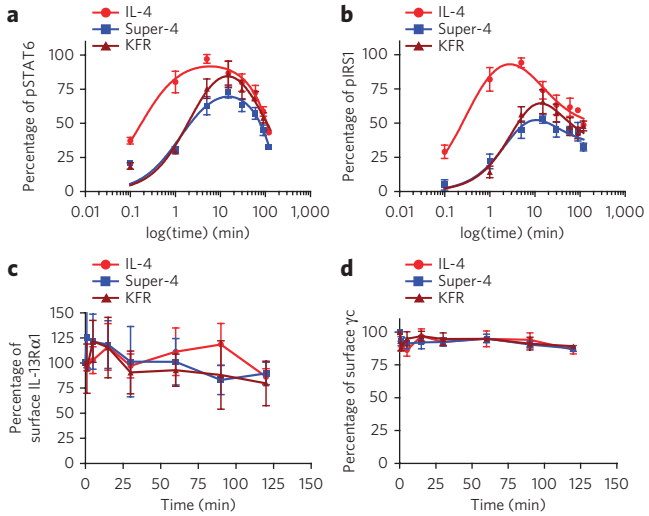

Figure 5 | Signaling and internalization kinetics of IL-4 and the two superkines in monocytes. CD14$^+$ monocytes (>97% pure) were stimulated with 30 pM of IL-4, super-4 or KFR for the indicated times. (**a**,**b**) Kinetics of STAT6 (**a**) and IRS1 phosphorylation (**b**) were measured by flow cytometry using phospho-specific antibodies coupled to fluorescence dyes. (**c**,**d**) Surface IL-13Rα1 (**c**) and γc internalization (**d**) were assayed by flow cytometry using fluorescently labeled receptor chain–specific antibodies. In both cases, data (mean ± s.e.m.) are from four healthy donors.

Signaling profile of IL-4 and superkines in monocytes

As IL-4 and the two superkines activated STAT6 to the same extent in monocytes (**Supplementary Fig. 6c**), we sought to understand why super-4 was unable to induce dendritic cell differentiation. Purified monocytes were treated with two doses of cytokines, one dose corresponding to the pSTAT6 half-maximum effective concentration (EC_{50}) value (30 pM) (**Fig. 5**) and another dose corresponding to saturation (50 nM) (**Supplementary Fig. 9**). The amount of STAT6 and IRS1 phosphorylation as well as the downregulation of the γc and IL-13Rα1 receptors were analyzed at the indicated times (**Fig. 5** and **Supplementary Fig. 9**). At low doses, super-4 and KFR showed delayed activation of STAT6 and IRS1 (**Fig. 5a**,**b**) when compared to IL-4. No major internalization of either γc or IL-13Rα1 was observed (**Fig. 5c**,**d**). At high doses, the three cytokines induced the same kinetics profile of STAT6 and IRS1 activation (**Supplementary Fig. 9a**,**b**). KFR showed stronger internalization of IL-13Rα1 at later times of stimulation (**Supplementary Fig. 9c**,**d**). Overall, these results show a lack of correlation between surface receptor internalization and signaling activation. Moreover, the delayed kinetics of signaling activation alone cannot explain the inefficiency of super-4 to induce dendritic cell differentiation, suggesting that type II receptor–specific signaling is required for dendritic cell differentiation.

Gene expression profiling of IL-4 and superkines

To gain qualitative insights into the extent of redundancy of genetic programs induced by IL-4 and superkines in differentiating dendritic cells, we performed genome-wide analysis of gene expression in response to wild-type IL-4 and the two superkines in monocytes treated simultaneously with GM-CSF. Monocytes from five healthy donors were stimulated for 6 h with GM-CSF with or without IL-4, KFR or super-4, and RNA expression was analyzed as described in Methods. As shown by scatter plot correlation, the three cytokines induce the vast majority of genes to the same extent (**Supplementary Fig. 10a**). However, notably, minor pockets of gene expression specificity can also be observed between IL-4 and the two superkines. A considerable number of genes were significantly ($P < 0.05$) induced by only one or two of the cytokines used. IL-4 specifically regulated 16 genes, whereas super-4 and KFR regulated 72 and 45 genes, respectively (**Supplementary Fig. 10b**). The heat map in **Supplementary Figure 10c** shows a representative set of cytokine-selective genes where clear differences in the expression patterns induced by IL-4 and the two superkines were observed. A more complete list of genes regulated differentially by superkines and IL-4 in monocytes is presented in **Supplementary Table 4**. Dendritic cell–specific genes such as *TPA1*, *HLA-DPA1* and *CISH* were clearly induced to a higher degree by IL-4 and KFR than by super-4, consistent with specific signals coming from the type II IL-4 receptor that could bias the dendritic cell differentiation process induced by IL-4.

Cytokine secretion profiling of IL-4 and superkines

To further assess the functionality of the dendritic cells induced by the engineered cytokines, we compared the secretion patterns of cytokines, chemokines and growth factors by performing a Luminex assay on supernatant of cells cultured for 8 d with or without lipopolysaccharide (LPS) stimulation during the last 24 h (**Fig. 6a**). Among the 51 analytes, 20 showed no difference in expression between treatments (superkines and LPS) (**Fig. 6b**), and 19 were upregulated by LPS (most notably IL-6, CCL3, CCL5 and CXCL1) without differences between IL-4 and the superkines (**Fig. 6c**). The expression of the remaining 12 products discriminated the cells induced by GM-CSF only or by GM-CSF plus super-4 from the dendritic cells induced by GM-CSF plus IL-4 or KFR (**Fig. 6d** and **Supplementary Fig. 11**). The former two subsets were very similar and produced more G-CSF, HGF, IL-1α, IL-1β, IL-10, IL-12p40, LIF and TNFα and less MCP3, MIP1β, PDGF and TGFα than the latter two, also very similar, subsets. Most of the differences were seen after LPS stimulation, but some also existed in nonactivated cells. Altogether, these data demonstrate that super-4 had no effect over that of GM-CSF alone on monocytes, whereas the addition of IL-4 or KFR led to phenotypically and functionally different dendritic cells. Thus, the engineered cytokines seem to have new and distinct functional activities.

DISCUSSION

Many cytokines being developed in the pharmaceutical sector are associated with dose-limiting toxicities or inadequate efficacy. One possibility for improving cytokines as pharmacologic agents is to bias them for preferential activity on certain desired cell types. Indeed, in a recent report by our lab, we succeeded in biasing the action of IL-2 to different leukocyte subsets by enhancing IL-2 affinity for IL-2Rβ[24]. Cytokines that act through heterodimeric receptor complexes, such as those in the γc, gp130 and βc families, are particularly amenable to this approach, given that the relative expression of the specific α chains of their receptors and the shared 'second' chains often vary on different cell types.

Here, guided by structures of IL-4 receptor complexes, we have altered the agonistic properties of IL-4 in a way to redirect cell subset selectivity through engineering based on the metric of differential second receptor chain expression. Though the signaling experiments qualitatively confirmed the superiority of super-4 over IL-4 for a cell line predominantly using the type I receptor (Ramos) and of KFR over IL-4 for a cell line predominantly using the type II receptor (A549), the differences between IL-4 and super-4 on Ramos cells or IL-4 and KFR on A549 cells were much less substantial than might have been anticipated. These results could be accounted for in several ways. The measurement of the equilibrium constant of the binding of soluble IL-4 (or superkine) complexed to IL-4Rα to immobilized γc or IL-13Rα1 may overestimate the differences in the two-dimensional equilibrium constants among these proteins for second chain recruitment on the cell surface when both ligand and receptor are membrane bound and have greater diffusion limits.

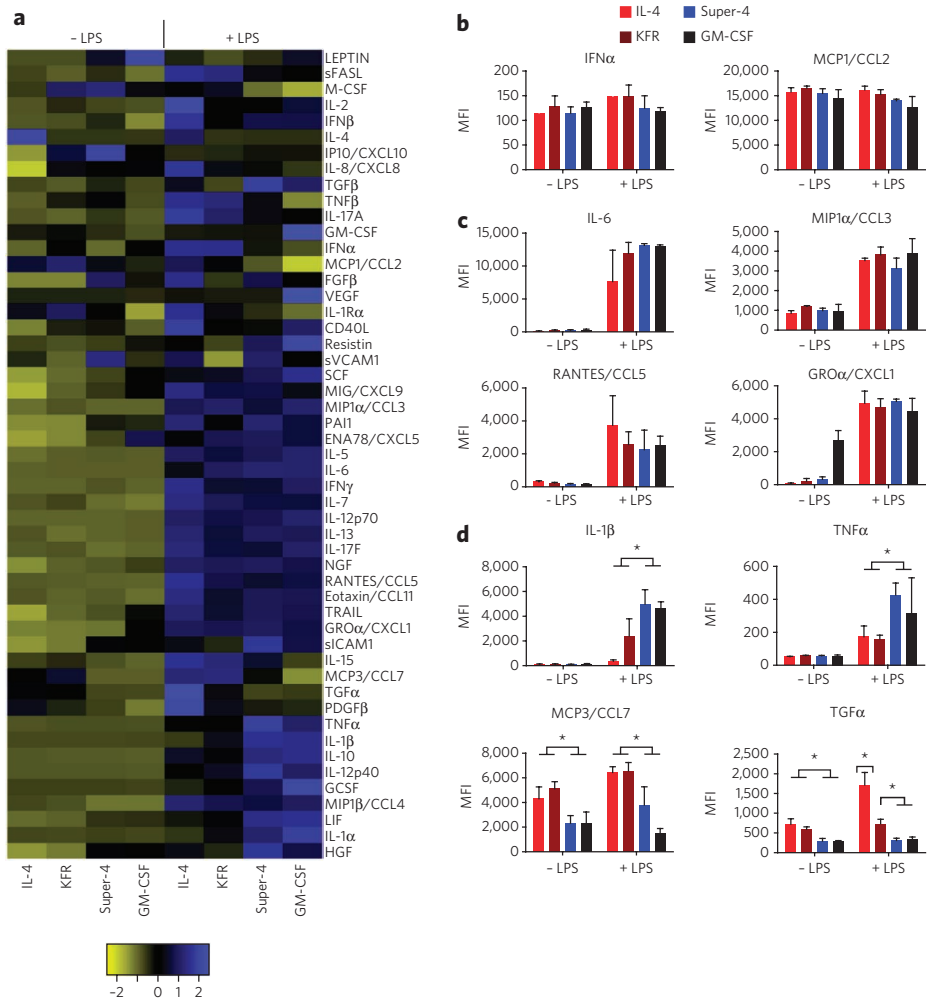

Figure 6 | Distinct patterns of cytokine secretion induced by IL-4 and the two superkines in immature and LPS-matured dendritic cells. Purified monocytes from three healthy donors were cultured for 7 d with GM-CSF (50 ng ml^{-1}) alone or combined with IL-4, KFR or super-4 (20 ng ml^{-1}), then stimulated (or not) with LPS (2 μg ml^{-1}) for another 24 h. (**a**) Culture supernatant was assessed by Luminex for relative amounts of 51 cytokines, chemokines and growth factors, as shown in heat map. (**b**–**d**) Representative examples of products whose secretion was either unchanged (IFNα and MCP1/CCL2; $n = 19$) (**b**), increased by LPS stimulation only (IL-6, MIP1α/CCL3, RANTES/CCL5 and GROα/CXCL1; $n = 20$) (**c**) or modulated by superkines in the presence or absence of LPS (IL-1β, TNFα, MCP3/CCL7 and TGFα; $n = 12$) (**d**). Data represent mean ± s.d. from three healthy donors (normalized to GM-CSF alone group). For all panels, $^*P < 0.05$; paired Student's *t*-test was used to determine significant changes.

Another possibility is that the receptor heterodimers could exist in a preassociated form or, alternatively, localize in membrane compartments in close proximity, as seen for IL-2 (ref. 25).

IL-4 is not currently in use as a therapeutic agent, but it had been considered for such use in the past and, if free of toxicity, might be considered for purposes such as directing CD4 T-cell differentiation during vaccination or altering an established pattern of differentiation in view of the recent recognition of the plasticity of differentiated CD4 T cells[26]. In the early 1990s, clinical trials were performed in which IL-4 was administrated to cancer patients with the hope of boosting T-cell responses or of engaging the innate immune system. However, intravenous administration of high doses (600 μg m^{-2} d^{-1}) of IL-4 resulted in a vascular leak syndrome in two out of three patients in the study group[27]. Other toxicities were encountered in these studies and in preclinical analysis. The production of IL-4 superkines that cannot activate the type II receptor or in which activation of the type I receptor can be achieved at substantially lower concentrations than activation of the type II receptor might mitigate these problems, as most nonhematopoietic cells use only the type II receptor, and cells of the monocyte or macrophage lineage tend to express similar numbers of both receptors. Indeed, our observation that super-4 was relatively inefficient in inducing dendritic cell differentiation favors this hypothesis and agrees with previous work describing the requirement of the type II IL-4 receptor for the surface expression of dendritic cell costimulatory molecules in mouse bone marrow precursor cells[28].

The use of IL-4 to redirect T-cell differentiation from more inflammatory phenotypes (such as T_H1 or T_H17) could be considered because CD4 T cells use the type I receptor virtually exclusively. Our data strongly suggest that super-4 would have greater efficacy for this purpose than IL-4 by combining a stronger activation of type I responses, which are required for T cell effects, and by reducing the activation of type II responses including dendritic cell differentiation. Indeed, super-4 more potently enhances T_H9 differentiation and may provide greater clinical benefit than IL-4 in boosting T_H9 immunity.

Whereas delivery of IL-4 by various means generally has a beneficial outcome in several preclinical models of autoimmunity, such as the nonobese diabetic or the collagen-induced arthritis mouse models, the interpretation of the mechanisms of action has been made difficult by the pleiotropic nature of IL-4 binding. Thus, the use of receptor-selective superkines in mouse models will help

to both better delineate the mode of action of therapies involving IL-4 and improve their efficacy[29,30].

The development of superkines can be considered as proof of the feasibility of this approach to achieve cell subset–specific cytokine effects. In principle, this approach can be attempted with many different cytokines whose signaling is dependent on the biophysical parameters of second chain recruitment.

METHODS

Details on protein expression, yeast surface display, biophysical analysis and microarray analysis are in **Supplementary Methods**.

Cell lines and stimulations with IL-4 and superkines. Ramos, U937, A549 and HH cells were grown in RPMI containing 10% v/v FBS, penicillin-streptomycin and L-glutamine (2 mM) and were maintained at 37 °C with 5% CO_2. Prior to stimulation, cells were cultured overnight in growth medium containing 2% v/v FBS ('starved'). For γc-blocking experiments, Ramos or U937 cells starved overnight were incubated for 1 h at 37 °C with blocking antibody (R&D).

Flow cytometric staining and antibodies. Cell surface expression of IL-4 receptor chains was performed after blocking Fc receptors I, II and III. Antibodies to CD23 (1:300 dilution) (no. 555711), IL-4Rα (1:300 dilution) (no. 552178) and γc (1:300 dilution) (no. 555900) were purchased from BD Biosciences, and an antibody to IL-13Rα1 (1:300 dilution) (no. FAB1462F) was purchased from R&D. Intracellular pSTAT6 (1:50 dilution) and pIRS-1 (1:50 dilution) staining was performed after ice-cold methanol (100% v/v) permeabilization. Antibodies to pSTAT6 Ax488 (anti–pSTAT6 Ax488; no. 612600) and pIRS-1 (anti–pIRS-1, no. 558440) were purchased from BD Biosciences. The induction of STAT6 phosphorylation was calculated by subtracting the MFI of the stimulated sample from that of the unstimulated sample. For primary human cells, analysis of STAT6 activation was performed as previously described[31]. Briefly, peripheral blood mononuclear cell (PBMC) samples from five donors were purified and stimulated with increasing concentrations of the appropriate cytokine for 15 min. Samples were then fixed in PFA for 15 min at 37 °C. Cells were pelleted, washed with PBS and permeabilized with cold (4 °C) methanol. Samples were then diluted with PBS to a final concentration of 50% and fluorescently barcoded with DyLight 800 and Pacific Orange dyes as previously described[31]. After barcoding and combining, samples were stained for 1 h with CD19 phycoerythrin (no. 302209), CD4 Brilliant Violet (no. 300531), CD14 PerCP-Cy5.5 (no. 325621) and CD8 phycoerythrin-Cy5 (no. 301009), which were purchased from Biolegend and used at 1:50 dilution, and anti-pSTAT6 Ax488. Analysis was performed on a BD Aria. Data analysis was performed in Cytobank software. Log MFI values were plotted against cytokine concentration to yield dose-response curves in cell subsets against pSTAT6.

RT-PCR. RNA was isolated from starved cells with RNeasy Kit (Qiagen). RNA was reverse-transcribed to cDNA using SuperScript II First-Strand Synthesis System for RT-PCR (Invitrogen). Quantitative PCR reactions were performed using a 7900HT sequence detection system (Applied Biosystems). The primer and probe sets to detect IL-4Rα, IL-13Rα1 and γc (FAM-MGB probe) and TaqMan Ribosomal RNA control reagents for detecting the 18S ribosomal RNA (VIC-MGB probe) were from Applied Biosystems. The mRNA levels were normalized to 18S ribosomal RNA.

T_H9 differentiation assay. Enriched CD4 T cells were prepared from buffy coats obtained from healthy donors (Stanford Blood Center) using RosetteSep Human $CD4^+$ T Cell Enrichment (Stem Cell Technologies) before density gradient centrifugation with Ficoll-Paque PLUS (GE Healthcare). Naive $CD4^+CD45RA^+CD45RO^-CD25^-$ T cells were magnetically sorted with Naive $CD4^+$ T Cell Isolation Kit II (Miltenyi Biotec). Cells were cultured at 37 °C in 48-well flat-bottomed plates (Falcon) in X-VIVO 15 medium (Lonza) supplemented with 10% v/v human serum type AB (Lonza), 100 U ml^{-1} penicillin-streptomycin, L-glutamine (Invitrogen) and 50 μM β-mercaptoethanol (Sigma-Aldrich). Cells were cultured at 2.5×10^5 cells per ml with anti-CD3– and anti-CD28–coated beads (Invitrogen) at a 1:1 bead-to-cell ratio in the presence of 5 ng ml^{-1} TGF-β (eBioscience) and the indicated concentrations of IL-4, super-4 or KFR (**Fig. 4a**). After 4 d in culture, beads were magnetically removed, and cells were restimulated with 25 ng ml^{-1} phorbol-12-myristate-13-acetate (PMA) and 750 ng ml^{-1} Ionomycin (Invitrogen) in the presence of brefeldin A (eBioscience) for 4 h. Cells were then stained with a LIVE/DEAD Fixable Aqua Dead Cell Stain Kit (Invitrogen), then fixed and permeabilized (eBioscience) according to the manufacturer's protocols. Subsequently, cells were stained with fluorescently labeled antibodies against IL-9 and Foxp3 (eBioscience). Labeled cells were acquired on a BD LSRII (BD Biosciences), and data were analyzed on gated live single cells by FlowJo software (Treestar).

Dendritic cell differentiation: phenotyping and cytokine profiling. $CD14^+$ monocytes were isolated (>97% purity) from PMBCs obtained from healthy blood donors (Stanford Blood Center) by density centrifugation using a RosetteSep Human Monocyte Enrichment Cocktail (Stem Cell Technologies) followed by magnetic separation with microbeads conjugated to antibodies against CD14 (Miltenyi Biotec). We subsequently cultured $0.5–1 \times 10^6$ $CD14^+$ monocytes with 50 ng ml^{-1} GM-CSF alone or with the indicated concentrations of IL-4, KFR or super-4 in 12-well plates (Corning) containing IMDM medium (Gibco) supplemented with 10% v/v human AB serum, 100 U ml^{-1} penicillin, 100 μg ml^{-1} streptomycin, 2 mM L-glutamine, sodium pyruvate, nonessential amino acids and 50 μM 2-mercaptoethanol. Fresh cytokines were added on days 2 and 4. Cells were processed between days 6 and 7 with 5 mM EDTA and subsequently stained with 4′,6-diamidino-2-phenylindole (DAPI; Invitrogen), fluorescently labeled antibodies against CD11c (no. 561356), CD16 (no. 560195), CD80 (no. 555683), CD86 (no. 555660), CD209 (no. 551265) and HLA-DR (no. 560944) (from BD Biosciences); CD1a (no. 8017-0017-025) and CD123 (no. 48-1239-42) (from eBioscience); CD1c (no. 331514), CD40 (no. 334312) and CD14 (no. 325619) (from Biolegend); and CD141 (no. 130-090-513) and CD304 (no. 130-090-9533) (from Miltenyi Biotec) or appropriate isotype controls. All the antibodies were use at 1:50 dilution. Dendritic cell differentiation was assessed by flow cytometry with a BD LSRII flow cytometer, and the MFI was determined on the FlowJo software (Treestar).

For Luminex cytokine profiling, culture supernatant was collected on day 8 (with or without 24-h stimulation with 2 μg ml^{-1} LPS). Human 51-plex kits were purchased from Affymetrix and used according to the manufacturer's recommendations with modifications as described below. Briefly, samples were mixed with antibody-linked polystyrene beads on 96-well filter-bottom plates and incubated at 25 °C for 2 h followed by overnight incubation at 4 °C. Plates were vacuum-filtered and washed twice with wash buffer and then were incubated with biotinylated detection antibody for 2 h at 25 °C. Samples were then filtered and washed twice as above and resuspended in streptavidin-phycoerythrin. After incubation for 40 min at 25 °C, two additional vacuum washes were performed, and the samples were resuspended in Reading Buffer (Affymetrix). Plates were read using a Luminex 200 instrument with a lower bound of 100 beads per sample per cytokine. MFI values were normalized to values from unstimulated cells cultured with GM-CSF only.

Accession codes. Protein Data Bank: crystal structure data for the IL-4 mutant RGA bound to γc is deposited under accession code 3QB7.

Received 15 May 2012; accepted 20 September 2012; published online 28 October 2012

References

1. Leonard, W.J. Type I cytokines and interferons and their receptors. in *Fundamental Immunology* (ed. Paul, W.) 741–774 (Lippinscott-Raven, Philadelphia, 1999).
2. Ihle, J.N. Cytokine receptor signalling. *Nature* **377**, 591–594 (1995).
3. Stroud, R.M. & Wells, J.A. Mechanistic diversity of cytokine receptor signaling across cell membranes. *Sci. STKE* **2004**, re7 (2004).
4. Wang, X., Lupardus, P., Laporte, S.L. & Garcia, K.C. Structural biology of shared cytokine receptors. *Annu. Rev. Immunol.* **27**, 29–60 (2009).
5. Cunningham, B.C. *et al.* Dimerization of the extracellular domain of the human growth hormone receptor by a single hormone molecule. *Science* **254**, 821–825 (1991).
6. LaPorte, S.L. *et al.* Molecular and structural basis of cytokine receptor pleiotropy in the interleukin-4/13 system. *Cell* **132**, 259–272 (2008).
7. Junttila, I.S. *et al.* Tuning sensitivity to IL-4 and IL-13: differential expression of IL-4Rα, IL-13Rα1, and γc regulates relative cytokine sensitivity. *J. Exp. Med.* **205**, 2595–2608 (2008).
8. Ito, T. *et al.* Distinct structural requirements for interleukin-4 (IL-4) and IL-13 binding to the shared IL-13 receptor facilitate cellular tuning of cytokine responsiveness. *J. Biol. Chem.* **284**, 24289–24296 (2009).
9. Mueller, T.D., Zhang, J.L., Sebald, W. & Duschl, A. Structure, binding, and antagonists in the IL-4/IL-13 receptor system. *Biochim. Biophys. Acta* **1592**, 237–250 (2002).
10. Nelms, K., Keegan, A.D., Zamorano, J., Ryan, J.J. & Paul, W.E. The IL-4 receptor: signaling mechanisms and biologic functions. *Annu. Rev. Immunol.* **17**, 701–738 (1999).
11. Kelly-Welch, A.E., Hanson, E.M., Boothby, M.R. & Keegan, A.D. Interleukin-4 and interleukin-13 signaling connections maps. *Science* **300**, 1527–1528 (2003).
12. Hage, T., Sebald, W. & Reinemer, P. Crystal structure of the interleukin-4/receptor α chain complex reveals a mosaic binding interface. *Cell* **97**, 271–281 (1999).
13. Andrews, A.L., Holloway, J.W., Holgate, S.T. & Davies, D.E. IL-4 receptor α is an important modulator of IL-4 and IL-13 receptor binding: implications for the development of therapeutic targets. *J. Immunol.* **176**, 7456–7461 (2006).
14. Andrews, A.L., Holloway, J.W., Puddicombe, S.M., Holgate, S.T. & Davies, D.E. Kinetic analysis of the interleukin-13 receptor complex. *J. Biol. Chem.* **277**, 46073–46078 (2002).
15. Heller, N.M. *et al.* Type I IL-4Rs selectively activate IRS-2 to induce target gene expression in macrophages. *Sci. Signal.* **1**, ra17 (2008).
16. Kraich, M. *et al.* A modular interface of IL-4 allows for scalable affinity without affecting specificity for the IL-4 receptor. *BMC Biol.* **4**, 13 (2006).

17. Wenzel, S., Wilbraham, D., Fuller, R., Getz, E.B. & Longphre, M. Effect of an interleukin-4 variant on late phase asthmatic response to allergen challenge in asthmatic patients: results of two phase 2a studies. *Lancet* **370**, 1422–1431 (2007).
18. Boder, E.T. & Wittrup, K.D. Yeast surface display for screening combinatorial polypeptide libraries. *Nat. Biotechnol.* **15**, 553–557 (1997).
19. Conrad, D.H. *et al.* Effect of B cell stimulatory factor-1 (interleukin 4) on Fcε and Fcγ receptor expression on murine B lymphocytes and B cell lines. *J. Immunol.* **139**, 2290–2296 (1987).
20. Siegel, J.P. & Mostowski, H.S. A bioassay for the measurement of human interleukin-4. *J. Immunol. Methods* **132**, 287–295 (1990).
21. Gavutis, M., Jaks, E., Lamken, P. & Piehler, J. Determination of the two-dimensional interaction rate constants of a cytokine receptor complex. *Biophys. J.* **90**, 3345–3355 (2006).
22. Wong, M.T. *et al.* Regulation of human T_H9 differentiation by type I interferons and IL-21. *Immunol. Cell Biol.* **88**, 624–631 (2010).
23. Dauer, M. *et al.* Mature dendritic cells derived from human monocytes within 48 hours: a novel strategy for dendritic cell differentiation from blood precursors. *J. Immunol.* **170**, 4069–4076 (2003).
24. Levin, A.M. *et al.* Exploiting a natural conformational switch to engineer an interleukin-2 'superkine'. *Nature* **484**, 529–533 (2012).
25. Pillet, A.H. *et al.* IL-2 induces conformational changes in its preassembled receptor core, which then migrates in lipid raft and binds to the cytoskeleton meshwork. *J. Mol. Biol.* **403**, 671–692 (2010).
26. O'Shea, J.J. & Paul, W.E. Mechanisms underlying lineage commitment and plasticity of helper CD4+ T cells. *Science* **327**, 1098–1102 (2010).
27. Sosman, J.A., Fisher, S.G., Kefer, C., Fisher, R.I. & Ellis, T.M. A phase I trial of continuous infusion interleukin-4 (IL-4) alone and following interleukin-2 (IL-2) in cancer patients. *Ann. Oncol.* **5**, 447–452 (1994).
28. Lutz, M.B. *et al.* Differential functions of IL-4 receptor types I and II for dendritic cell maturation and IL-12 production and their dependency on GM-CSF. *J. Immunol.* **169**, 3574–3580 (2002).
29. Creusot, R.J. *et al.* A short pulse of IL-4 delivered by DCs electroporated with modified mRNA can both prevent and treat autoimmune diabetes in NOD mice. *Mol. Ther.* **18**, 2112–2120 (2010).
30. Creusot, R.J. *et al.* Tissue-targeted therapy of autoimmune diabetes using dendritic cells transduced to express IL-4 in NOD mice. *Clin. Immunol.* **127**, 176–187 (2008).
31. Krutzik, P.O. & Nolan, G.P. Fluorescent cell barcoding in flow cytometry allows high-throughput drug screening and signaling profiling. *Nat. Methods* **3**, 361–368 (2006).

Acknowledgments

The authors thank J. Gregorio and K. Weiskopf for assistance and the Stanford Human Immune Monitoring Center. This work was supported by US National Institute of Allergy and Infectious Diseases Division of Intramural Research (I.S.J. and W.E.P.), the Finnish Medical Foundation, the Sigrid Juselius Foundation (I.S.J.), the Howard Hughes Medical Institute (K.C.G.), the US National Institutes of Health (NIH) RO1-AI51321 (K.C.G.) and NIH UO1-DK078123 (C.G.F.) and the Stanford Immunology Program Training Grant (D.L.B.).

Author contributions

K.C.G. conceived the project, designed approaches for engineering of IL-4 and initiated subsequent cellular and functional experiments. D.L.B. and P.L. performed protein engineering and biophysical experiments. I.S.J., R.J.C., I.M. and W.E.P. designed and performed signaling experiments. R.J.C., M.M.-S. and I.M. performed transcriptional analysis and Luminex experiments. W.E.P., I.S.J. and M.M.S. performed mathematical modeling using Matlab. M.T.W., M.N.A., M.M.S. and I.M. performed dendritic cell experiments. I.S.J., R.J.C., I.M., D.L.B., C.G.F., P.J.U., W.E.P. and K.C.G. analyzed the data. P.J.U. and E.G.E. provided reagents and guidance for human primary cell experiments. I.S.J., R.J.C., I.M., W.E.P. and K.C.G. wrote the manuscript.

Competing financial interests

The authors declare no competing financial interests.

Additional information

Supplementary information is available in the online version of the paper. Reprints and permissions information is available online at http://www.nature.com/reprints/index.html. Correspondence and requests for materials should be addressed to K.C.G.